

An elementary introduction to the geometry of quantum states with a picture book

J. Avron, O. Kenneth

Dept. of Physics, Technion, Israel

December 15, 2024

Abstract

This is a review of the geometry of quantum states using elementary methods and pictures. Quantum states are represented by a convex body, often in high dimensions. In the case of n -qubits, the dimension is exponentially large in n . The space of states can be visualized, to some extent, by its simple cross sections: Regular simplexes, balls and hyper-octahedra¹. When the dimension gets large there is a precise sense in which the space of states resembles, almost in every direction, a ball. The ball turns out to be a ball of rather low purity states. We also address some of the corresponding, but harder, geometric properties of separable and entangled states and entanglement witnesses..

“All convex bodies behave a bit like Euclidean balls.”
Keith Ball

Contents

1	Introduction	2
1.1	The geometry of quantum states	2
1.2	The geometry of separable states	7
2	Two qubits	9
2.1	Numerical sections for 2 qubits	9
2.2	A 3-D section through Bell states	10

¹Also known as cross polytope, orthopex, and co-cube

3	Basic geometry of Quantum states	12
3.1	Choosing coordinates	12
3.2	Most of the unit sphere does not represent states	14
3.3	Inversion asymmetry	14
3.4	The inscribed sphere	14
4	Cross sections	15
4.1	Cross sections that are N-1 simplexes	16
4.2	Cross sections that are balls	17
4.3	Cross sections that are polyhedra and hyper-octahedra	17
4.4	2D cross sections in the Pauli basis	18
5	The radius function	18
5.1	The radius function is N-Lifshitz	19
6	A tiny ball in most directions	20
6.1	Application of random matrix theory	20
6.2	Directions associated with states with substantial purity are rare . .	22
7	Separable and entangled states	23
7.1	Why separability is hard	23
7.2	Completely separable simplex: Classical bits	24
7.3	Entangled pure states	25
7.4	Two types of entangled states	26
7.5	The largest ball of bi-partite separable states	27
7.6	Entanglement witnesses	28
7.7	Entangled states and witnesses near the Gurvits-Barnum ball . . .	29
7.8	A Clifford ball of separable states	31
A	The average purity of quantum states	33
B	The N dimensional unit cube is almost a ball	34
	References	36

1 Introduction

1.1 The geometry of quantum states

The set of states of a single qubit is geometrically a ball, the Bloch ball [1]: The

density matrix ρ is 2×2 :

$$\rho(\mathbf{x}) = \frac{\mathbb{1} + \mathbf{x} \cdot \boldsymbol{\sigma}}{2}, \quad \mathbf{x} \in \mathbb{R}^3, \quad (1.1)$$

with $\boldsymbol{\sigma} = (\sigma_1, \sigma_2, \sigma_3)$, the vector of 2×2 (Hermitian, traceless) Pauli matrices. $\rho \geq 0$, provided $|\mathbf{x}| \leq 1$. The unit sphere, $|\mathbf{x}|^2 = 1$, represents pure states where ρ is a rank one projection. The interior of the ball describes mixed states and the center of the ball the fully mixed state, (Fig. 1).

The geometry of a qubit is not always a good guide to the geometry of general quantum states: n -qubits *are not* represented by n Bloch balls², and quantum states are not, in general, a ball in high dimensions.

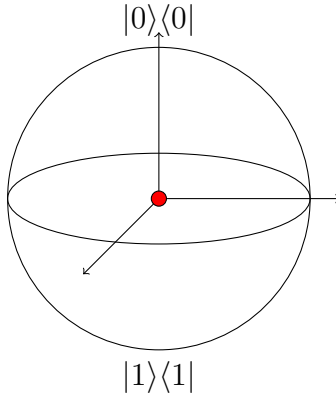


Figure 1: The Bloch ball representation of a qubit: The unit sphere represents the pure states and its interior the mixed states. The fully mixed state is the red dot. Orthogonal states are antipodal.

Quantum states are mixtures of pure states. We denote the set of quantum state in an $N \geq 2$ dimensional Hilbert space by D_N :

$$D_N = \left\{ \rho \left| \rho = \sum_{j=1}^k p_j |\psi_j\rangle \langle \psi_j|, p_j \geq 0, \sum_j p_j = 1, |\psi_j\rangle \in \mathbb{C}^N, \|\psi_j\| = 1 \right. \right\} \quad (1.2)$$

The representation implies:

- The quantum states form a convex set.
- The pure states are its extreme points. As we shall see in section 3.2, the set of pure states is a smooth manifold, which is a tiny subset of ∂D_N when N is large.

² n Bloch balls describe uncorrelated qubits.

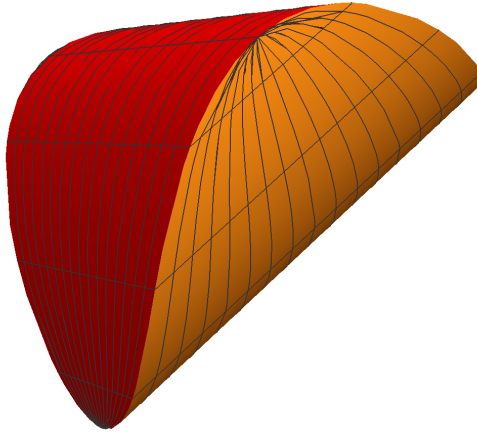


Figure 2: The figure shows a three dimensional convex body whose geometry shares some of the qualitative features of D_N (and S_{N_1, \dots, N_k}): The extreme points lie on a low dimensional smooth sub-manifold of the boundary at fixed distance from the center and lack inversion symmetry.

- The spectral theorem gives (generically) a distinguished decomposition with $k \leq \dim \mathcal{H}$.

Fig. 2 shows a three dimensional body whose geometry reflects better the geometry of the space of states D_N for general N , (and also the spaces of separable states), than the Bloch sphere does.

Choosing a basis in \mathcal{H} , the state ρ is represented by a positive $N \times N$ matrix with unit trace ($N = \dim \mathcal{H} \geq 2$). In the case of n -qubits $N = 2^n$. Since the sum of two positive matrices is a positive matrix, the positive matrices form a convex cone in \mathbb{R}^{N^2} , and the positive matrices with unit trace are a slice of this cone. The slice is an $N^2 - 1$ dimensional convex body with the pure states $|\psi\rangle\langle\psi|$ as its extreme points and the fully mixed state as its “center of mass”.

The geometric properties of D_N can be complicated and, because of the high dimensions involved, counter-intuitive. Even the case of two qubits, where D_N is 15 dimensional, is difficult to visualize [2, 3, 4, 5].

In contrast with the complicated geometry of D_N , the geometry of equiva-

lence classes of quantum states under unitaries, even for large N , is simple: It is parametrized by eigenvalues and represented by the $N - 1$ -simplex, Fig. 3,

$$1 \geq \rho_1 \geq \dots \geq \rho_N \geq 0, \quad \sum \rho_j = 1$$

All pure states are represented by the single extreme point, $(1, 0, \dots, 0)$, and the fully mixed state by the extreme point $(1, \dots, 1)/N$. The equivalence classes corresponding to the Bloch ball are represented by an interval (1-simplex) which corresponds to the radius of the Bloch ball.

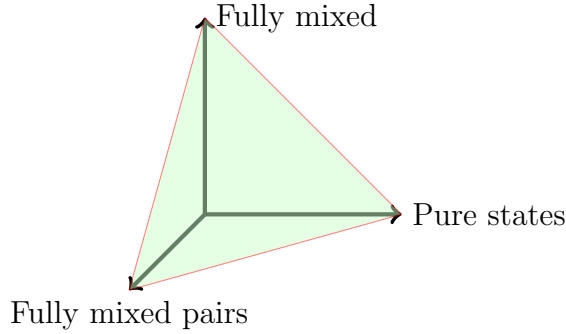


Figure 3: The equivalence classes of qutrits make a triangle.

Clearly, the geometry of D_N does not resemble the geometry of the set of equivalence classes: The two live in different dimensions, have different extreme points and D_N is, of course, not a polytope.

One of the features of a qubit that holds for any D_N , is that the pure states are equidistant from the fully mixed state. Indeed

$$\text{Tr} \left(|\psi\rangle \langle\psi| - \frac{\mathbb{1}}{N} \right)^2 = 1 - \frac{1}{N} \quad (1.3)$$

However, the converse is not true. In fact, the largest ball inscribed in D_N is the Gurvits-Barnum ball³ [6]:

$$B_{gb} = \left\{ \rho \left| \text{Tr} \left(\rho - \frac{\mathbb{1}}{N} \right)^2 \leq \frac{1}{N-1} - \frac{1}{N} \right. \right\} \quad (1.4)$$

It follows that:

•

$$\dim D_N = N^2 - 1$$

³Gurvits and Barnum define the radius of the ball by its purity, rather than the distance from the maximally mixed states.

- Since⁴

$$\frac{\text{radius of bounding ball of } D_N}{\text{radius of inscribed ball of } D_N} = N - 1 \quad (1.5)$$

only D_2 is a ball and D_N gets increasingly far from a ball when N is large, Fig. 4.

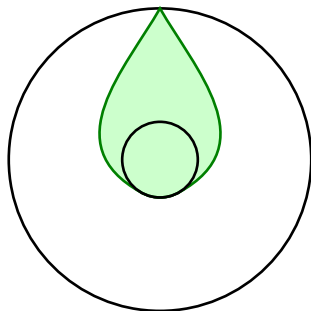


Figure 4: The inscribed, Gurvits-Barnum, ball is represented by the small circle and the bounding sphere by the large circle. The green area represents D_N .

Another significant difference between a single qubit and the general case is that D_N is inversion symmetric only for $N = 2$. Indeed, inversion with respect to the fully mixed state is defined by

$$I(\rho) = \frac{\mathbb{1}}{N} - \left(\rho - \frac{\mathbb{1}}{N} \right) = \frac{2}{N} \mathbb{1} - \rho \quad (1.6)$$

Evidently I is trace preserving and $I^2 = 1$. However, it is not positivity preserving in general. $I(\rho) \geq 0$ implies that

$$0 \leq \text{Tr}(\rho I(\rho)) = \frac{2}{N} - \text{Tr}(\rho^2) \quad (1.7)$$

A matrix ρ and its inversion $I(\rho)$ can not both be states unless the purity of ρ is small enough.

The low symmetry together with the large aspect ratio indicate that the geometry of D_N may be complicated. It can be visualized, to some extent, by looking at cross sections. As we shall see D_N has several cross sections that are simple to describe: Regular simplexes, balls and hyper-octahedra.

D_N has a Yin-Yang relation to spheres in high dimensions: As N gets large D_N gets increasingly far from a ball as is evidenced by the diverging ratio of

⁴The balls are centered at the mixed state which is the natural “center of mass” of all states.

the bounding sphere to the inscribed ball. At the same time there is a sense in which the converse is also true: Viewed from the center (the fully mixed state), the distance to ∂D_N , is the same for almost all directions. In this sense, D_N increasingly resembles a ball. The radius of the ball can be easily computed using standard facts from random matrix theory [7], and we find that as $N \rightarrow \infty$, for almost all directions,

$$2NT\text{Tr} \left(\rho - \frac{\mathbb{1}}{N} \right)^2 \rightarrow 1, \quad \rho \in \partial D_N \quad (1.8)$$

The fact that D_N is almost a ball is not surprising. In fact, a rather general consequence of the theory of “concentration of measures”, [8, 9, 10], is that sufficiently nice high dimensional convex bodies are essentially balls⁵. D_N , however, is not sufficiently nice so that one can simply apply standard theorems from concentration of measure. Instead, we use information about the second moment of D_N and Hölder inequality to show that the set of directions θ that allow for states with significant purity has super-exponentially small measure (see section 6.2).

1.2 The geometry of separable states

The Hilbert space of a quantum system partitioned into n groups of (distinguishable) particles has a tensor product structure $\mathcal{H} = \mathcal{H}_{N_1} \otimes \cdots \otimes \mathcal{H}_{N_n}$. The set of separable states of such a system, denoted $S_{N_1 \dots N_n}$, is defined by [12],

$$S_{N_1 \dots N_n} = \left\{ \rho \left| \rho = \sum_{j=1}^k p_j \left| \psi_j^{(1)} \right\rangle \left\langle \psi_j^{(1)} \right| \otimes \cdots \otimes \left| \psi_j^{(n)} \right\rangle \left\langle \psi_j^{(n)} \right|, \left| \psi_j^{(m)} \right\rangle \in \mathcal{H}_{N_m} \right\} \quad (1.9)$$

where p_j are probabilities.

For reasons that we shall explain in section 7, $S_{N_1 \dots N_n}$ are more difficult to analyze than D_N . They have been studied by many authors from different perspectives [5, 9, 6, 2]. It will be a task with diminishing returns to try and make a comprehensive list of all of the known results. Selected few references are [3, 4, 9, 13, 11, 14, 15, 16, 17]. We shall review, instead, few elementary observations and accompany them by pictures.

The representation in Eq. (1.9) implies that

- $S_{N_1 \dots N_n} \subseteq D_N$ where $N = \prod_j N_j$
- $S_{N_1 \dots N_n}$ is a convex set with pure-product states as its extreme points.

⁵Applications of concentration of measure to quantum information are given in e.g. [6, 9, 11].

- The finer the partition the smaller the set

$$S_{N_1, N_2, N_3} \subseteq S_{N_1, N_2 \times N_3} \cap S_{N_3, N_1 \times N_2} \cap S_{N_2, N_1 \times N_3}$$

Strict inclusion implies that Alice, Bob and Charlie may have a 3-body entanglement that is not visible in any bi-partite partition.

- By Caratheodory theorem, one can always find a representation with $k \leq N^2$ in Eq. (1.9). In the case of two qubits a results of Wootters [18] gives $k \leq N$.
- $S_{N_1 \dots N_n}$ is invariant under partial transposition, (transposition of any one of its factor), i.e.

$$\left| \psi_j^{(m)} \right\rangle \left\langle \psi_j^{(m)} \right| \mapsto \left(\left| \psi_j^{(m)} \right\rangle \left\langle \psi_j^{(m)} \right| \right)^t \quad (1.10)$$

- The bounding sphere of $S_{N_1 \dots N_n}$ is the bounding sphere of D_N .
- The separable states are of full measure:

$$\dim S_{N_1, \dots, N_n} = N^2 - 1 \quad (1.11)$$

It is enough to show this for the maximally separable set. For simplicity, consider the case of n qubits. For each qubit $\mathbb{1} + \sigma_\mu$ with $\mu = 1, \dots, 3$ are linearly independent and positive. The same is true for their tensor products. This gives $4^n = N^2$ linearly independent separable states spanning a basis in the space of Hermitian matrices.

By a result of [6]:

$$B_{gb} \subseteq S_{N_1, N_2} \quad (1.12)$$

for any partition. It implies that:

- Since⁶

$$\frac{\text{radius of bounding ball of } S_{N_1, N_2}}{\text{radius of inscribed ball of } S_{N_1, N_2}} = N - 1 \quad (1.13)$$

the separable states get increasingly far from a ball when N is large.

We expect that the separable states too are approximated by balls in most direction, but unlike the case of D_N , we do not know how to estimate the radii of these balls.

⁶See footnote 4.

2 Two qubits

Two qubits give a much better intuition about the geometry of general quantum states than a single qubit. However, as 2 qubits live in 15 dimensions, they are still hard to visualize.

One way to gain insight into the geometry of two qubits is to consider equivalence classes that can be visualized in 3 dimensions [19, 2, 4, 20]). However, as we have noted above, the geometry of equivalence classes is distinct from the geometry of states. An alternate way to visualize 2 qubits is to look at 2 and 3 dimensional cross sections through the space of states.

Let's parameterize the states of two by $\mathbf{x} \in \mathbb{R}^{15}$ where $\mathbf{x} = (x_{01}, \dots, x_{33})$

$$\rho(\mathbf{x}) = \frac{\mathbb{1}_4 + \sqrt{3} (\sum_{\mu\nu=01}^{33} x_{\mu\nu} \sigma_\mu \otimes \sigma_\nu)}{4}, \quad (2.1)$$

σ_μ are the Pauli matrices. By a 2 dimensional section in the space of two qubits we mean a two dimensional plane in \mathbb{R}^{15} going through the origin.

2.1 Numerical sections for 2 qubits

The 2 dimensional figures 5 and 6 show random sections obtained by numerically testing the positivity and separability of ρ , using Mathematica. A generic plane will miss the pure states, which are a set of lower dimension. This situation is shown in Fig. 5.

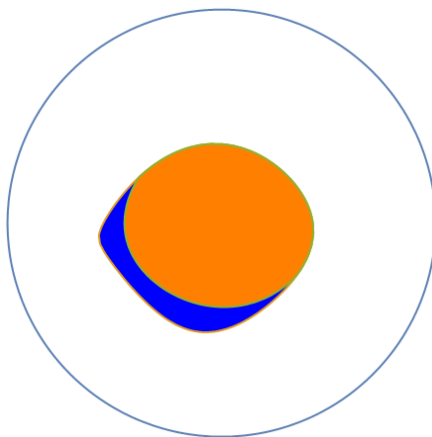


Figure 5: A numerical computation of a random planar cross section through the origin in the space of 2 qubits. The orange spheroid shows the separable states and the blue moon the entangled states. The orange spheroid is not too far from a sphere centered at the origin.

Fig. 6 shows a two dimensional section obtained by picking two pure states randomly. Since a generic pure state is entangled, the section goes through two pure entangled states lying on the unit circle.

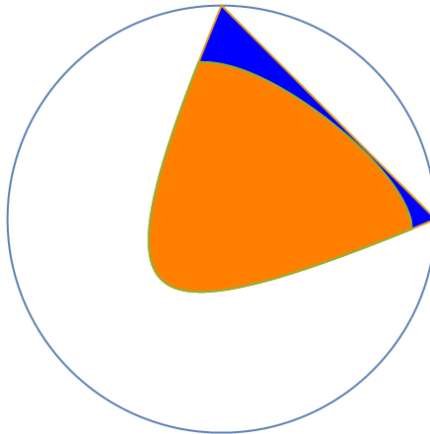


Figure 6: A numerical computation of a planar cross section through the origin and through two random pure states (located on the circle). The orange region shows the separable states and the blue region the entangled states. The section is quite far from a sphere centered at the origin.

2.2 A 3-D section through Bell states

Consider the 3D cross section given by⁷:

$$4\rho(x, y, z) = \mathbb{1} + \sqrt{3}(x\sigma_1 \otimes \sigma_1 + y\sigma_2 \otimes \sigma_2 + z\sigma_3 \otimes \sigma_3) \quad (2.2)$$

The section has the property that both subsystems are maximally mixed

$$\text{Tr}_2 \rho = \text{Tr}_1 \rho = \frac{\mathbb{1}}{2}$$

Since the purity is given by

$$\text{Tr}(\rho^2) = \frac{1}{4} + \frac{3}{4}(x^2 + y^2 + z^2) \quad (2.3)$$

the pure states lie on the unit sphere and all the states in this section must lie inside the unit ball.

The matrices on the right commute and satisfy one relation

$$(\sigma_1 \otimes \sigma_1)(\sigma_2 \otimes \sigma_2) = -\sigma_3 \otimes \sigma_3$$

⁷A generic two qubits state is SLOCC equivalent to a point of this section, see [4].

It follows that $\rho \geq 0$ iff (x, y, z) lie in the intersection of the 4 half spaces:

$$x \pm y \mp z \geq -\frac{1}{\sqrt{3}}, \quad -x \pm y \pm z \geq -\frac{1}{\sqrt{3}} \quad (2.4)$$

This defines a regular tetrahedron with vertices

$$\frac{1}{\sqrt{3}}(1, 1, -1), \quad \frac{1}{\sqrt{3}}(1, -1, 1), \quad \frac{1}{\sqrt{3}}(-1, 1, 1), \quad \frac{1}{\sqrt{3}}(-1, -1, -1) \quad (2.5)$$

The vertices of the tetrahedron lie at the corners of the cube in Fig. 7, at unit distance from the origin. It follows that the vertices of the tetrahedron represent pure states. As the section represents states with maximally mixed subsystems, the four pure states are maximally entangled: They are the 4 Bell states

The pairwise averages of the four corners of the tetrahedron give the $\binom{4}{2} = 6$ vertices of the octahedron in Fig. (7). By Eq. (7.10) below, these averages represent separable states. It follows that the octahedron represents separable states.

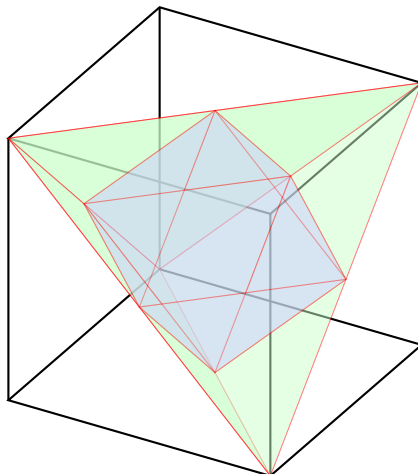


Figure 7: A 3D cross section in the space of states of 2 qubits. The 4 Bell states lie at the vertices of the tetrahedron of states. The octahedron shows the separable states. The vertices of the cube represent the extreme points of the, trace normalized, entanglement witnesses. The cube is inscribed in the unit sphere (not shown).

The cube, being the dual of the octahedron, represents the trace-normalized entanglement witnesses (see section 7.6). If \mathbf{s} is a vector inside the octahedron and \mathbf{w} a vector inside the cube then

$$0 \leq Tr(W\rho_s) = \frac{1 + 3\mathbf{s} \cdot \mathbf{w}}{4} \quad (2.6)$$

3 Basic geometry of Quantum states

3.1 Choosing coordinates

Any Hermitian $N \times N$ matrix with unit trace can be written as:

$$\rho(\mathbf{x}) = \frac{\mathbb{1}_N + \sqrt{N-1} \mathbf{x} \cdot \boldsymbol{\sigma}}{N}, \quad \mathbf{x} \in \mathbb{R}^{N^2-1} \quad (3.1)$$

$\mathbb{1}_N = \sigma_0$ is the identity matrix and $\boldsymbol{\sigma} = (\sigma_1, \dots, \sigma_{N^2-1})$ a vector of N^2-1 traceless, Hermitian, mutually orthogonal, $N \times N$ matrices

$$\text{Tr}(\sigma_\alpha \sigma_\beta) = \delta_{\alpha\beta} N, \quad \alpha, \beta \in \{1, \dots, N^2-1\} \quad (3.2)$$

This still leaves considerable freedom in choosing the coordinates σ_α and one may impose additional desiderata. For example:

- σ_α are either real symmetric or imaginary anti-symmetric

$$\sigma_\alpha^t = \pm \sigma_\alpha \quad (3.3)$$

This requirement is motivated by $\rho \geq 0 \iff \rho^t \geq 0$

- σ_α for $\alpha \neq 0$ are unitarily equivalent, i.e. are iso-spectral.

A coordinate system that has these properties in $N = 2^n$ dimensions, is the (generalized) Pauli coordinates:

$$\sigma_\mu = \sigma_{\mu_1} \otimes \dots \otimes \sigma_{\mu_n}, \quad \mu_j \in \{0, \dots, 3\}, \quad \mu \in \{1, \dots, N^2-1\} \quad (3.4)$$

σ_μ are iso-spectral with eigenvalues ± 1 . This follows from:

$$\sigma_\mu^2 = \mathbb{1}_N, \quad \text{Tr} \sigma_\mu = 0 \quad (3.5)$$

The Pauli coordinates behave nicely under transposition:

$$\sigma_\mu^t = \pm \sigma_\mu \quad (3.6)$$

In addition, they either commute or anti-commute

$$\sigma_\mu \sigma_\beta = \pm \sigma_\beta \sigma_\mu. \quad (3.7)$$

This will prove handy in what follows. One drawback of the Pauli coordinates is that they only apply to Hilbert spaces with special dimensions, namely $N = 2^n$.

For N arbitrary, one may not be able satisfy all the desiderata simultaneously. In particular, the standard basis

$$X_{jk} = |j\rangle \langle k| + |k\rangle \langle j|, \quad Y_{jk} = i(|j\rangle \langle k| - |k\rangle \langle j|), \quad Z_{jN} = |j\rangle \langle j| - |N\rangle \langle N| \quad (3.8)$$

is iso-spectral with eigenvalues $\{\pm 1, 0\}$ and behave nicely under transposition. However, the Z_{jN} coordinates are not mutually orthogonal.

With a slight abuse of notation we redefine

$$D_N = \left\{ \mathbf{x} \mid \rho(\mathbf{x}) \geq 0 \right\} \quad (3.9)$$

Note that the Hilbert space and the Euclidean distances are related by scaling

$$N \text{Tr}(\rho - \rho')^2 = (N - 1) (\mathbf{x} - \mathbf{x}')^2 \quad (3.10)$$

The basic geometric properties of D_N follow from Eq. (1.2):

- The fully mixed state, $\mathbb{1}/N$, is represented by the origin $\mathbf{x} = 0$
- The pure states lie on the unit sphere for all N . This follows either from Eqs. (1.3, 3.10) or, alternatively, from a direct computation of the purity:

$$p = \text{Tr}(\rho^2) = \frac{1}{N} + \left(1 - \frac{1}{N}\right) |\mathbf{x}|^2 \quad (3.11)$$

- Since the pure states are the extreme points of D_N :

$$D_N \subseteq B_1 = \left\{ \mathbf{x} \mid |\mathbf{x}| \leq 1 \right\} \quad (3.12)$$

- Since $\rho \geq 0 \iff \rho^t \geq 0$ D_N is symmetric under reflection of the “odd” coordinates associated with the anti-symmetric matrices.
- Since there is no reflection symmetry for the “even” Pauli coordinates, $\sigma_\alpha = \sigma_\alpha^t$, one does not expect D_N to have inversion symmetry in general (as we have seen in Eq. (1.7)).

Let θ be a point on the unit sphere in \mathbb{R}^{N^2-1} and (r, θ) be the polar representation of \mathbf{x} , in particular $r = |\mathbf{x}|$. Denote by $r(\theta)$ the radius function of D_N , i.e. the distance from the origin of the boundary of D_N in the θ direction. Then

$$1 \geq r(\theta) = -\frac{r_0}{\lambda_1(\theta)} > 0, \quad 1 \geq r_0 = \frac{1}{\sqrt{N-1}} \geq 0 \quad (3.13)$$

where $\lambda_1(\theta) < 0$ is the smallest eigenvalue of

$$S(\theta) = \boldsymbol{\theta} \cdot \boldsymbol{\sigma} \quad (3.14)$$

3.2 Most of the unit sphere does not represent states

For $N = 2$, every point of the unit sphere represents a pure state, however, for $N \geq 3$ this is far from being the case. In fact, $\rho(\mathbf{x})$ of Eq. (3.1) is not a positive matrix for most $\mathbf{x}^2 = 1$. This follows from a simple counting argument: Pure states can be written as $|\psi\rangle\langle\psi|$ with $|\psi\rangle$ a normalized vector in \mathbb{C}^N . It follows that

$$\dim_{\mathbb{R}}(\text{pure states}) = 2(N - 1) \quad (3.15)$$

while

$$\dim\left(\text{unit sphere in } \mathbb{R}^{N^2-1}\right) = N^2 - 2 \quad (3.16)$$

When $N \geq 3$ pure states make a small subset of the of the unit sphere. When N is large the ratio of dimensions is arbitrarily small.

Since (pure) states make a tiny subset of the unit sphere, spheres with radii close to 1, should be mostly empty of states. In section 6.2 we shall give a quantitative estimate of this observation.

3.3 Inversion asymmetry

The Hilbert space and the Euclidean space scalar products are related by

$$N \text{Tr}(\rho\rho') = 1 + (N - 1)(\mathbf{x} \cdot \mathbf{x}') \quad (3.17)$$

The positivity of $\text{Tr}\rho\rho' \geq 0$ and Eq. (3.17) say that if both \mathbf{x} and \mathbf{x}' correspond to bona-fide states then it must be that

$$\mathbf{x} \cdot \mathbf{x}' \geq -\frac{1}{N - 1}, \quad \mathbf{x}, \mathbf{x}' \in D_N \quad (3.18)$$

In particular, no two pure states are ever related by inversion if $N \geq 3$.

3.4 The inscribed sphere

The inscribed ball in D_N , the Gurvits-Barnum ball, is

$$B_{gb} = \left\{ \mathbf{x} \left| |\mathbf{x}| \leq \frac{1}{N - 1} \right. \right\} \subseteq D_N \quad (3.19)$$

It is easy to see that the inscribed ball is at most the Gurvits-Barnum ball since the state

$$\tau_\psi = \frac{\mathbb{1} - |\psi\rangle\langle\psi|}{N - 1} \quad (3.20)$$

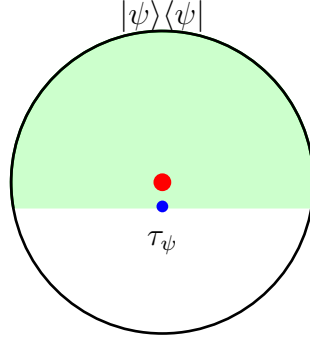


Figure 8: The figure shows the intersection of the half space in Eq. (3.18) with the unit ball in the case that \mathbf{x} corresponds to a pure state $|\psi\rangle$. The blue dot represents the state τ_ψ of Eq. (3.20).

clearly lies on ∂D_N . Using Eq. (3.17), one verifies that $|\mathbf{x}_\psi| = \frac{1}{N-1}$ saturating Eq. (3.19).

Eq. (3.19) follows from:

$$\begin{aligned} B_{gb} &= \left\{ \mathbf{x} \left| \mathbf{x} \cdot \mathbf{x}' \geq -\frac{1}{N-1}, |\mathbf{x}'| \leq 1 \right. \right\} \\ &\subseteq \left\{ \mathbf{x} \left| \mathbf{x} \cdot \mathbf{x}' \geq -\frac{1}{N-1}, \mathbf{x}' \in D_N \right. \right\} \\ &\subseteq D_N \end{aligned} \tag{3.21}$$

In the last step we used the fact that the positivity of ρ follows from the positivity of ρ' by Eq. (3.17).

Remark 3.1. *An alternate proof is: By Eq. (3.13) minimizing $r(\theta)$ is like minimizing the smallest eigenvalue $\lambda_1(\theta)$ of $S(\theta) = \boldsymbol{\theta} \cdot \boldsymbol{\sigma}$ under the constraints $\text{Tr} S^2(\theta) = N$ and $\text{Tr} S(\theta) = 0$. The minimum occurs when*

$$\text{spec}(S) = \left(-\frac{1}{r_0}, r_0, \dots, r_0 \right), \quad r_0 = \frac{1}{\sqrt{N-1}}$$

This, together with Eq. (3.13), gives r_0^2 for the radius of the inscribed ball of non-negative matrices.

4 Cross sections

D_N has few sections that are simple to describe, even when N is large.

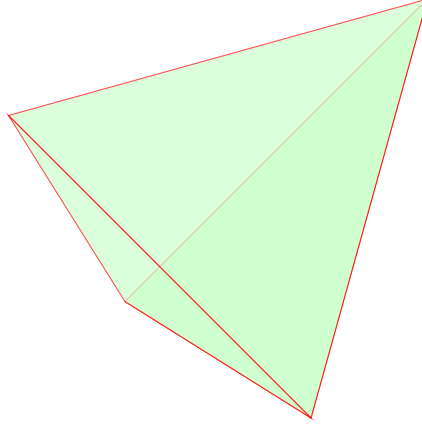


Figure 9: Any basis of pure states for 2 qubits and in particular, the Bell states and the computational basis are represented by the vertices of a three dimensional tetrahedron. These simplexes are three dimensional cross sections of D_2 .

4.1 Cross sections that are $N-1$ simplexes

Let \mathbf{v}_j , with $j = 0, \dots, N-1$ be the (unit) vectors associated with pure states $\rho_j = |\psi_j\rangle\langle\psi_j|$ corresponding to the orthonormal basis $\{|\psi_j\rangle\}$. Using Eq. (3.17) we find for $\text{Tr}\rho_j\rho_k = \delta_{jk}$

$$\mathbf{v}_j \cdot \mathbf{v}_k = \frac{N\delta_{jk} - 1}{N-1} \quad (4.1)$$

For a single qubit, $N = 2$, orthogonal states are (annoyingly) represented by antipodal points on the Bloch sphere. The situation improves when N gets large: Orthogonal states are represented by almost orthogonal vectors. Moreover, from Eq. (3.1)

$$\sum_{j=0}^{N-1} \rho_j = \mathbb{1} \iff \sum_{j=0}^{N-1} \mathbf{v}_j = 0 \quad (4.2)$$

The N vectors \mathbf{v}_j define a regular $(N-1)$ -simplex, centered at the origin (in \mathbb{R}^{N^2-1})

$$C_{N-1} = (\mathbf{v}_0, \dots, \mathbf{v}_{N-1}) \quad (4.3)$$

Since the boundary of C_{N-1} represent states that are not full rank, it belongs to the boundary of D_N and therefore is an $N-1$ slice of D_N .

4.2 Cross sections that are balls

Suppose $N = 2^n$. Consider the largest set of mutually anti-commuting matrices among the $N^2 - 1$ (generalized) Pauli matrices σ_α . Since the Pauli matrices include the matrices that span a basis of a Clifford algebra we have at least ℓ anti-commuting matrices

$$\{\sigma_j, \sigma_k\} = 2\delta_{jk}, \quad j, k \in \{1, \dots, \ell\}, \quad \ell = n + 2 \left\lfloor \frac{n+1}{2} \right\rfloor \quad (4.4)$$

For the anti-commuting σ_j we have

$$\left(\sum x_j \sigma_j \right)^2 = r^2 = \sum x_j^2 \quad (4.5)$$

The positivity of

$$\mathbb{1}_N + \sqrt{N-1} \sum_{j=1}^{\ell} x_j \sigma_j \geq 0 \quad (4.6)$$

holds iff

$$r \leq r_0 = \frac{1}{\sqrt{N-1}}$$

This means that D_N has ℓ dimensional cross sections that are perfect balls⁸. This result extends to $2^n \leq N < 2^{n+1}$.

4.3 Cross sections that are polyhedra and hyper-octahedra

Consider the set of commuting matrices σ_α . Since the matrices can be simultaneously diagonalized, there are $N - 1$ of them and the positivity condition on the cross-section

$$\mathbb{1} + \sqrt{N-1} \sum_{\alpha=1}^{N-1} x_\alpha \sigma_\alpha \geq 0$$

reduces to a set of linear inequalities for x_α . This defines a polyhedron.

In the case of n qubits, a set of n commuting σ_α matrices with no relations is:

$$\sigma_\alpha = \mathbb{1} \otimes \dots \otimes \mathbb{1} \otimes \sigma_x \otimes \mathbb{1} \cdots \otimes \mathbb{1}, \quad j = \alpha, \dots, n$$

The cross section is the intersection of N half-spaces

$$\pi_\alpha \cdot x \geq -r_0, \quad \alpha = 1, \dots, N, \quad \pi_\alpha \in \{-1, 1\}^n$$

The corresponding cross section is a regular n dimensional hyper-octahedron⁹: A regular, convex polytope with n vertices and $N = 2^n$ hyper-planes. (The dual of the n dimensional cube.)

⁸This and section 6 are reminiscent of Dvoretzki-Milman theorem [10].

⁹See footnote 1.

4.4 2D cross sections in the Pauli basis

Any two dimensional cross section along two Pauli coordinates can be written as:

$$N\rho(x, y) = \mathbb{1}_N + \sqrt{N-1}(x\sigma_\alpha + y\sigma_\beta) \quad (4.7)$$

By Eq. (3.7), $\sigma_{\alpha,\beta}$ either commute or anti-commute. The case that they anti-commute is a special case of the Clifford ball of section 4.2 where positivity implies

$$x^2 + y^2 \leq r_0^2 = \frac{1}{N-1}$$

The case that $\sigma_{\alpha,\beta}$ commute is a special case of section 4.3 where positivity holds if

$$|x| + |y| < r_0 \quad (4.8)$$

Both are balls, albeit in different metrics, (ℓ^2 and ℓ^1), see Fig. 10.

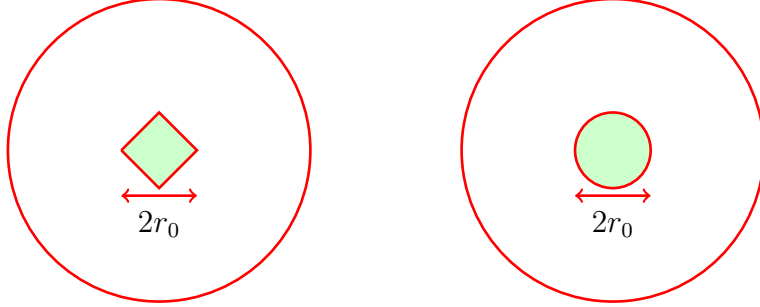


Figure 10: A two dimensional cross sections of the space of states of n qubits, D_n , along the Pauli coordinates, $(\sigma_\alpha, \sigma_\beta)$, is either a tiny square or a tiny disk both of diameter $2r_0$.

5 The radius function

By a general principle: “All convex bodies in high dimensions are a bit like Euclidean balls” [21]. More precisely, consider a convex body C_N in N dimensions, which contains the origin as an interior point. The radius function of C_N is called K-Lifshitz, if

$$|r(\theta) - r(\theta')| \leq K\|\theta - \theta'\| \quad (5.1)$$

By a standard result in the theory of concentration of measure [21, 8], the radius is concentrated near its median, with a variance that is at most $O(K^2/N)$ [21].

D_N is a convex body in $N^2 - 1$ dimensions. As we shall see in the next section, $r(\theta)$ turns out to be N -Lifshitz. As a consequence, the variance of the distribution

of the radius about the mean is only guaranteed to be $O(1)$. This is not strong enough to conclude that D_N is almost a ball.

5.1 The radius function is N-Lifshitz

Since D_N is convex and $r(\theta) > 0$, the radius function is continuous, but not necessarily differentiable. The fact that D_N is badly approximated by a ball is reflected in the continuity properties of $r(\theta)$.

Using the notation of section 4.1, let C_j be the simplex

$$C_j = \{\mathbf{v}_0, \dots, \mathbf{v}_j\} \quad (5.2)$$

C_j , for $j < N - 1$, is a face of C_{N-1} . Denote by \bar{C}_j the bary-center of C_j ,

$$\bar{C}_j = \frac{1}{j+1} \sum_{\alpha=0}^j \mathbf{v}_\alpha, \quad (5.3)$$

$\bar{C}_{N-1} = 0$ represents the fully mixed state, by Eq. (4.2).

The three points \bar{C}_0, \bar{C}_{N-2} and \bar{C}_{N-1} define a triangle, shown in Fig. 11. The sides of the triangle can be easily computed, e.g.

$$\bar{C}_0 - \bar{C}_{N-1} = \bar{C}_0 = \mathbf{v}_0 \implies |\bar{C}_0 - \bar{C}_{N-1}| = 1 \quad (5.4)$$

Since \mathbf{v}_0 represents a pure state. Similarly

$$\bar{C}_{N-2} - \bar{C}_{N-1} = \bar{C}_{N-2} = -\frac{1}{N-1} \mathbf{v}_{N-1} \implies |\bar{C}_{N-2} - \bar{C}_{N-1}| = \frac{1}{N-1} \quad (5.5)$$

Consider the path from \bar{C}_{N-2} to \bar{C}_0 . The path lies on the boundary of D_N . Therefore $r(\theta)$ in the figure is the radius function. By the law of sines

$$r(\theta) = \frac{\sin \alpha}{\sin(\alpha + \theta)} \quad (5.6)$$

and

$$\left| \frac{r'(\theta)}{r(\theta)} \right| = |\cot(\alpha + \theta)| \implies |r'(0)| = \cot \alpha = \frac{N^2 - 2N + 2}{\sqrt{N(N-2)}} \approx N \quad (5.7)$$

It follows that when N is large, the radius function has large derivatives near the vertices of the simplex. This reflects the fact that locally D_N is not well approximated by a ball.

Remark 5.1. One can show that $\text{Max } |r'(\theta)| \leq O(N)$ is tight. But we shall not pause to give the proof here.

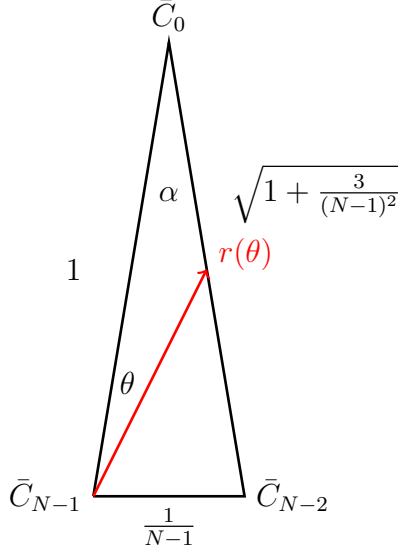


Figure 11: The radius $r(\theta)$ along the path from \bar{C}_{N-2} to \bar{C}_0 has large derivative, $O(N)$, near $\theta = 0$.

6 A tiny ball in most directions

A basic principle in probability theory asserts that while anything that might happen will happen as the system gets large, certain features can become regular, universal, and non-random [22]. As N gets large, D_N , in most directions, is a ball, whose radius is

$$r_t \approx \frac{r_0}{2} \quad (6.1)$$

Although the radius of the ball is small when N is large, it is much larger than the inscribed ball whose radius is r_0^2 . The computation of r_t is a simple application of random matrix theory [7].

6.1 Application of random matrix theory

Define a random direction $\boldsymbol{\theta}$ by a vector of iid Gaussian random variables:

$$\boldsymbol{\theta} = (\theta_1, \dots, \theta_{N^2-1}), \quad \theta_\alpha \sim \mathcal{N}\left[0, \frac{1}{N^2-1}\right] \quad (6.2)$$

where $\mathcal{N}[\mu, \sigma^2]$ denotes the normal distribution with mean μ and variance σ^2 . $\boldsymbol{\theta}$ has mean unit length

$$\mathbb{E}(|\boldsymbol{\theta}|^2) = (N^2 - 1)\mathbb{E}(\theta_1^2) = 1$$

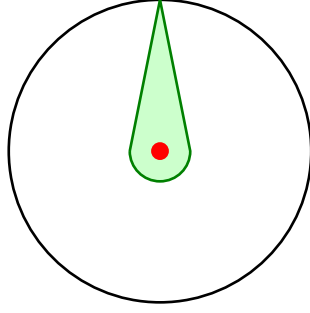


Figure 12: D has, in most direction, a small radius, and extends to the pure states only in rare direction.

and small variance

$$\begin{aligned}\mathbb{E} \left((|\boldsymbol{\theta}|^2 - 1)^2 \right) &= -1 + \sum_{\alpha\beta} \mathbb{E} (\theta_\alpha^2 \theta_\beta^2) \\ &= \frac{2}{N^2 - 1}\end{aligned}$$

$S(\boldsymbol{\theta}) = \boldsymbol{\theta} \cdot \boldsymbol{\sigma}$ may be viewed as an element of the ensemble of the $N \times N$ traceless Hermitian random matrices.

By Wigner semi-circle law, when N is large, the density μ of eigenvalues approach a semi-circle

$$d\mu = \frac{2}{\pi\Lambda^2} \sqrt{\Lambda^2 - \lambda^2} d\lambda \quad (6.3)$$

with edges at

$$\Lambda^2 = \frac{4}{N} \mathbb{E} (Tr (S^2(\boldsymbol{\theta}))) = 4 \quad (6.4)$$

When N is large, the bottom of the spectrum, $\lambda_1(\boldsymbol{\theta})$, a random variable, is close to the bottom edge at -2 [23]. The radius function $r(\theta)$ is related to the lowest eigenvalue $\lambda_1(\boldsymbol{\theta})$ by Eq. (3.13) and the value for r_t in Eq. (6.1) follows¹⁰.

Remark 6.1. *To see where the value of Λ comes from, observe that by Eq. (6.3)*

$$\mathbb{E} (Tr (\boldsymbol{\theta} \cdot \boldsymbol{\sigma})^2) = \sum_j \mathbb{E} (\lambda_j^2) \approx N \int \lambda^2 d\mu = N \frac{\Lambda^2}{4} \quad (6.5)$$

¹⁰Since $\boldsymbol{\theta}$ is a unit vector only on average, there is a slight relative ambiguity in r . The error is smaller than the $N^{-2/3}$ fluctuation in the Tracy-Widom distribution [23].

6.2 Directions associated with states with substantial purity are rare

Our aim in this section is to show that the probability for finding directions where $r(\theta) \geq r_0$ is exponentially small.¹¹ More precisely:

$$\text{Prob}(r \geq a) \leq \left(\frac{r_0}{a}\right)^{N^2+1} \quad (6.6)$$

In particular, states that lie outside the sphere of radius r_0 have super-exponentially small measure in the space of directions.

To see this, let $d\mu$ be a (normalized) measure on D_N . From Eq. (3.11) we get a relations between the average purity and the average radius¹²:

$$\int_{D_N} \text{Tr}(\rho^2) d\mu = \frac{1}{N} + \left(1 - \frac{1}{N}\right) \int_{D_N} r^2 d\mu \quad (6.7)$$

In the special case that $d\mu$ is proportional to the Euclidean measure in \mathbb{R}^{N^2-1} , the lhs is known exactly [24]:

$$\frac{1}{|D_N|} \int_{D_N} \text{Tr}(\rho^2) dx_1 \dots dx_{N^2-1} = \frac{2N}{N^2+1} \quad (6.8)$$

This gives for the *radius of inertia*

$$r_e^2 = \int_{D_N} r^2 d\mu = \frac{N+1}{N^2+1} \quad (6.9)$$

We use this result to estimate the probability of rare direction that accommodate states with substantial purity. From Eq. (6.9) we have

$$\frac{N+1}{N^2+1} = \frac{\int_{D_N} d\Omega dr r^2 r^{N^2-2}}{\int_{D_N} d\Omega dr r^{N^2-2}} = \frac{(N^2-1) \int_{D_N} d\Omega r^{N^2+1}(\boldsymbol{\theta})}{(N^2+1) \int_{D_N} d\Omega r^{N^2-1}(\boldsymbol{\theta})} \quad (6.10)$$

Cancelling common terms we find

$$\frac{1}{N-1} = \frac{\int_{D_N} d\Omega r^{N^2+1}(\boldsymbol{\theta})}{\int_{D_N} d\Omega r^{N^2-1}(\boldsymbol{\theta})} \quad (6.11)$$

¹¹Note that $r_0 = 2r_t$ with r_t the radius of the ball determined by random matrix theory. This is an artefact of the method we use where r_e plays a role. When N is large $r_0 \approx r_e$. The stronger result should have r_0 replaced by r_t in Eq. (6.6).

¹²In Appendix A we show how to explicitly compute the average purity for measures obtained by partial tracing.

By Hölder inequality

$$\int_{D_N} d\Omega r^{N^2-1} \leq \left(\int_{D_N} d\Omega r^{(N^2-1)p} \right)^{1/p} \left(\int_{D_N} d\Omega 1^q \right)^{1/q} \quad (6.12)$$

Picking

$$p = \frac{N^2 + 1}{N^2 - 1}, \quad q = \frac{N^2 + 1}{2}$$

gives

$$\int d\Omega r^{N^2-1} \leq \left(\int d\Omega r^{N^2+1} \right)^{1/p} \left(\int d\Omega \right)^{1/q} \quad (6.13)$$

And hence,

$$r_0^2 = \frac{1}{N-1} = \frac{\int d\Omega r^{N^2+1}}{\int d\Omega r^{N^2-1}} \geq \left(\frac{\int d\Omega r^{N^2+1}}{\int d\Omega} \right)^{1/q}$$

It follows that

$$r_0^{N^2+1} \geq \frac{\int d\Omega r^{N^2+1}}{\int d\Omega} \geq a^{N^2+1} \text{Prob}(r \geq a)$$

This gives Eq. (6.6).

Remark 6.2. The inequality Eq. (6.6) gives an upper bound on r_t :

$$r_t^2 < r_0^2 + O(1/N^3)$$

which is independent of random matrix theory, but weaker by factor 2.

7 Separable and entangled states

7.1 Why separability is hard

Testing whether ρ is a state involves testing the positivity of its eigenvalues. The cost of this computation is polynomial in N . Testing whether ρ is separable is harder. Properly formulated, it is known to be NP-hard, see e.g. the review [25]. Algorithms that attempt to decide whether ρ is separable or not have long running times.

A pedestrian way to see why separability might be a hard decision problem is to consider the toy problem of deciding whether a given point $\mathbf{x} \in \mathbb{R}^d$ lies inside a polygon. The polygon is assumed to contain the origin and is given as

the intersection of M half-spaces, each of which contains the origin. This can be formulated as¹³

$$\mathbf{c}_\alpha \cdot \mathbf{x} \leq 1, \quad \alpha = 1, \dots, M$$

To decide if a point \mathbf{x}' belongs to the polygon, one needs to test M inequalities. The point is that M can be very large even if d is not. For example, in the poly-octahedron $M = 2^d$ and the number of inequalities one needs to check is exponentially large in d .

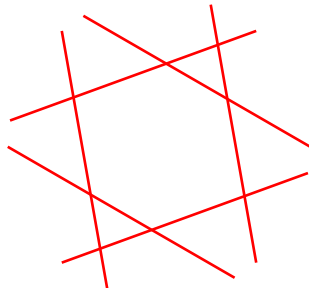


Figure 13: A hexagon defined by the intersection of six half-planes.

Locating a point in a high-dimensional polygon is related to testing for separability [14]: The separable states can be approximated by a polyhedron in \mathbb{R}^{N^2-1} whose vertices are chosen from a sufficiently fine mesh of pure product states. Since the number M of half-spaces could, in the general case, be exponentially large in N . Testing for separability becomes hard.

Myrheim et. al. [3] gave a probabilistic algorithm that, when successful, represents the input state as a convex combination of product states, and otherwise gives the distance from a nearby convex combination of product states. The algorithm works well for small N and freely available as web applet [26].

7.2 Completely separable simplex: Classical bits

The computational basis vectors are pure products, and are the extreme points of a completely separable $(N - 1)$ -simplex ($N = 2^n$). The computational states represent classical bits corresponding to diagonal density matrices:

$$\rho = \text{diagonal}(\rho_0, \dots, \rho_{N-1}), \quad 1 \geq \rho_\alpha \geq 0, \quad \sum \rho_\alpha = 1 \quad (7.1)$$

The simplex is interpreted as the space of probability distributions for classical n bits strings: ρ_α is the probability of the n -bits string $\alpha \in \{0, \dots, N - 1\}$.

¹³ \mathbf{c}_α is, in general, not normalized to 1.

7.3 Entangled pure states

Pure bi-partite states can be put into equivalence classes labeled by the Schmidt numbers, [1], leading to a simple geometric description.

Write the bipartite pure state in $\mathbb{C}^{N_1} \otimes \mathbb{C}^{N_2}$, ($N_1 \leq N_2$), in the Schmidt decomposition [1],

$$|\psi\rangle = \sum_{j=0}^{N_1-1} \sqrt{p_j} |\phi_j\rangle \otimes |\chi_j\rangle, \quad \langle \phi_j | \phi_k \rangle = \langle \chi_j | \chi_k \rangle = \delta_{jk} \quad (7.2)$$

with $p_j \geq 0$ probabilities. The simplex

$$1 \geq p_0 \geq \dots \geq p_{N_1-1} > 0, \quad \sum p_j = 1 \quad (7.3)$$

has the pure product state as the extreme point

$$(1, 0, \dots, 0) \quad (7.4)$$

All other points of the simplex represent entangled states. The extreme point

$$\frac{1}{N_1}(1, 1, \dots, 1) \quad (7.5)$$

is the maximally entangled state. Most pure states are entangled. (In contrast to the density matrix perspective, where by Eq. (1.11), the separable states are of full dimension.)

The maximally entangled state is, ($N_1 = M$ to simplify the notation):

$$|\beta\rangle = \frac{1}{\sqrt{M}} \sum_{j=0}^{M-1} |j\rangle \otimes |j\rangle \quad (7.6)$$

Let σ_μ be M^2 hermitian and mutually orthogonal $M \times M$ matrices i.e.

$$\sigma_\mu = \sigma_\mu^*, \quad \text{Tr} \sigma_\mu \sigma_\nu = M \delta_{\mu\nu}, \quad \mu \in 0, \dots, M^2 - 1 \quad (7.7)$$

The projection on $|\beta\rangle$ can be written in terms of σ_μ as:

$$\begin{aligned}
|\beta\rangle\langle\beta| &= \frac{1}{M} \sum_{jk=0}^{M-1} |jj\rangle\langle kk| \\
&= \frac{1}{M^3} \sum_{jk=0}^{M-1} \sum_{\mu,\nu=0}^{M^2-1} \langle kk| \sigma_\mu \otimes \sigma_\nu^t |jj\rangle \sigma_\mu \otimes \sigma_\nu^t \\
&= \frac{1}{M^3} \sum_{\mu,\nu=0}^{M^2-1} \text{Tr}(\sigma_\mu \sigma_\nu) \sigma_\mu \otimes \sigma_\nu^t \\
&= \frac{1}{M^2} \sum_{\mu=0}^{M^2-1} \sigma_\mu \otimes \sigma_\mu^t
\end{aligned} \tag{7.8}$$

In the case of qubits and $N = M^2$, a complete set of mutually orthogonal projections on the N maximally entangled states is:

$$P_\alpha = \frac{1}{N} \sum_{\mu=0}^{N^2-1} \sigma_\alpha \sigma_\mu \sigma_\alpha \otimes \sigma_\mu^t, \quad \alpha \in 0, \dots, N-1 \tag{7.9}$$

This is a natural generalization of the Bell basis of two qubits, to $2n$ qubits.

In the two qubits case, $M = 2$, an equal mixture of two Bell states, is a separable state:

$$\begin{aligned}
P_\alpha + P_0 &= \frac{1}{4} \sum_{\mu=0}^3 (\sigma_\alpha \sigma_\mu \sigma_\alpha + \sigma_\mu) \otimes \sigma_\mu^t \\
&= \frac{1}{2} (\sigma_0 \otimes \sigma_0 + \sigma_\alpha \otimes \sigma_\alpha^t) \\
&= \frac{\sigma_0 + \sigma_\alpha}{2} \otimes \frac{\sigma_0 + \sigma_\alpha^t}{2} + \frac{\sigma_0 - \sigma_\alpha}{2} \otimes \frac{\sigma_0 - \sigma_\alpha^t}{2}
\end{aligned} \tag{7.10}$$

The two terms on the last line are products of one dimensional projections, and represent together a mixture of pure product states.

7.4 Two types of entangled states

Choosing the basis σ_α made with either symmetric real or anti-symmetric imaginary matrices, makes partial transposition a reflection in the anti-symmetric coordinates

$$(\sigma_\alpha \otimes \sigma_\beta)^{pt} = \sigma_\alpha \otimes \sigma_\beta^t = \pm \sigma_\alpha \otimes \sigma_\beta \tag{7.11}$$

Partial transposition [27, 1] distinguishes between two types of entangled states:

- $\rho \geq 0$ while ρ^{pt} is not a positive matrix.
- Both $\rho, \rho^{pt} \geq 0$ but ρ is not separable.

In the case that ρ is a pure state or¹⁴ $N_1 N_2 \leq 6$, only the first type exists [16].

The Peres¹⁵ entanglement test [27] checks the non-positivity of ρ^{pt} and uncovers entangled state of the first type. Local operations can not convert states of the second kind into states of the first kind since positivity of partial transposition of ρ implies the positivity under partial transposition of a local operation

$$(M \otimes N)\rho(M^* \otimes N^*) \quad (7.12)$$

In particular, one can not distill Bell pairs from entangled states of the second kind by local operations. This is the reason why states of the second kind are called “bound entangled”: The Bell pairs used to produced them can not be recovered.

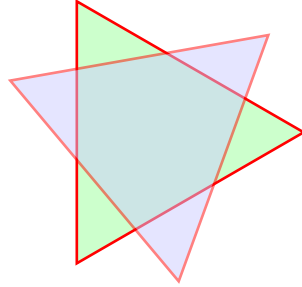


Figure 14: The green triangle represent a high dimensional simplex of states and the blue triangle and its partial transposition. The green triangles that stick out describe entangled states that are discoverable by partial transposition. The intersection may or may not contain bound entangled states. It is separable iff its vertices are separable.

7.5 The largest ball of bi-partite separable states

The Gurvits-Barnum ball was introduced in section 3.4 as the largest inscribed ball in D_N :

$$B_{gb} = \left\{ \mathbf{x} \mid |\mathbf{x}| \leq r_0^2 \right\} \subseteq D_N \quad (7.13)$$

Since partial transposition is a reflection in the σ_α coordinates, and any sphere centered at the origin is invariant under reflection, we have that

$$B_{gb} \subseteq D_N \cap D_N^{pt} \quad (7.14)$$

¹⁴Simple geometric proofs for two qubits are given in [3, 4].

¹⁵Gurvits and Barnum attribute the test to an older 1976 paper of Woronowicz. Apparently, nothing is ever discovered for the first time (M. Berry’s law).

B_{gb} therefore does not contain entangled states that are discoverable by the Peres test.

Gurvits and Barnum replace partial transposition by contracting positive maps of the form $\mathbb{1} \otimes \phi(D)$ to show [6], that B_{gb} is a ball of bi-partite separable states

$$B_{gb} \subseteq S_{N_1, N_2} \quad (7.15)$$

7.6 Entanglement witnesses

An entanglement witness for a given partition, (N_1, \dots, N_n) , is a Hermitian matrix W so that

$$\text{Tr}(W\rho) \geq 0 \quad \forall \quad \rho \in S_{N_1, \dots, N_n} \quad (7.16)$$

This definition makes the set of witnesses a convex cone.

Remark 7.1. *We consider $W \geq 0$ a witness even though it is “dumb” as it does not identify any entangled state. This differs from the definition used in various other places where witnesses are required to be non-trivial, represented by an indefinite W . Non-trivial witnesses have the drawback that they do not form a convex cone.*

The inequality, Eq (7.16), is sharp for ρ in the interior of S_{N_1, \dots, N_n} . As the fully mixed state belongs to the interior

$$\text{Tr}(W) = \text{Tr}(W \mathbb{1}) > 0 \quad (7.17)$$

we may normalize witnesses to have a unit trace and represent them, alongside the states, by

$$W(\mathbf{w}) = \frac{\mathbb{1}_N + \sqrt{N-1} \mathbf{w} \cdot \boldsymbol{\sigma}}{N}, \quad \mathbf{w} \in \mathbb{R}^{N^2-1} \quad (7.18)$$

We shall show that:

$$\text{Bi-partite witnesses} \subseteq B_1 = \left\{ \mathbf{x} \mid |\mathbf{x}| \leq 1 \right\} \quad (7.19)$$

This follows from

$$N \text{Tr}(W\rho) = 1 + (N-1) \mathbf{x} \cdot \mathbf{w} \quad (7.20)$$

and

$$\begin{aligned} \text{Bi-partite witnesses} &= \left\{ \mathbf{w} \mid \mathbf{x} \cdot \mathbf{w} \geq -\frac{1}{N-1} \quad \forall \mathbf{x} \in S_{N_1, N_2} \right\} \\ &\subseteq \left\{ \mathbf{w} \mid \mathbf{x} \cdot \mathbf{w} \geq -\frac{1}{N-1} \quad \forall \mathbf{x} \in B_{gb} \right\} \\ &= B_1 \end{aligned} \quad (7.21)$$

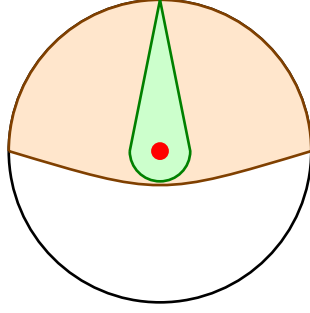


Figure 15: The separable states (green) and the corresponding witnesses, (Schematic).

Example 7.1. A witness for the partitioning $N = N_1 N_2$, $N_1 N_2 \geq M > 1$, is:

$$S = \sum_{j,k=1}^M |j\rangle \langle k| \otimes |k\rangle \langle j| \quad (7.22)$$

S is indeed an entanglement witness since

$$\langle \psi \otimes \phi | S | \psi \otimes \phi \rangle = \left| \sum_{j=1}^M \langle \psi | j \rangle \langle j | \phi \rangle \right|^2 \geq 0 \quad (7.23)$$

Since $\text{Tr } S = M$, the corresponding normalized witness is

$$W_S = \frac{S}{M} = (|\beta\rangle \langle \beta|)^{pt} \quad (7.24)$$

and the equality on the right follows from the first line of Eq. (7.8).

Since partial transposition is an isometry, it is clear that W_S lies at the same distance from the maximally mixed state as the pure state $|\beta\rangle \langle \beta|$. In particular, the associated vector \mathbf{w}_S lies on the unit sphere.

Remark 7.2. In the case that the partitioning is to two isomorphic Hilbert spaces, $N_1 = N_2$, S is the swap. In a coordinate free notation

$$S |\psi\rangle \otimes |\psi\rangle = |\phi\rangle \otimes |\phi\rangle \quad (7.25)$$

$|\beta\rangle$ is then the Bell state.

7.7 Entangled states and witnesses near the Gurvits-Barnum ball

Near the boundary of B_{gb} one can find entangled states and (non-trivial) entanglement witnesses, see Fig. (16).

To see this, consider the bi-partitionning $N = M^2$. Since $S^2 = \mathbb{1}$ and $S = S^*$,

$$P_S = \frac{\mathbb{1} + S}{2}, \quad P_A = \frac{\mathbb{1} - S}{2} \quad (7.26)$$

are orthogonal projections. P_S projects on the states that are symmetric under swap, and P_A on the anti-symmetric ones. Hence,

$$\text{Tr } P_A = \frac{M(M-1)}{2}, \quad \text{Tr } P_S = \frac{M(M+1)}{2} \quad (7.27)$$

The state

$$\rho = \frac{1+\varepsilon}{M(M-1)}P_A + \frac{1-\varepsilon}{M(M+1)}P_S, \quad 0 < \varepsilon \leq 1 \quad (7.28)$$

is entangled with the swap as witness. Indeed,

$$\begin{aligned} \text{Tr}(S\rho) &= \frac{1+\varepsilon}{M(M-1)}\text{Tr}(SP_A) + \frac{1-\varepsilon}{M(M+1)}\text{Tr}(SP_S) \\ &= -\frac{1+\varepsilon}{M(M-1)}\text{Tr}(P_A) + \frac{1-\varepsilon}{M(M+1)}\text{Tr}(P_S) \\ &= -\frac{1+\varepsilon}{2} + \frac{1-\varepsilon}{2} = -\varepsilon \end{aligned} \quad (7.29)$$

When ε is small, ρ is close to the Gurvits-Barnum ball. One way to see this is to compute its purity

$$\begin{aligned} \text{Tr}\rho^2 &= \left(\frac{1+\varepsilon}{M(M-1)}\right)^2 \text{Tr}P_A + \left(\frac{1-\varepsilon}{M(M+1)}\right)^2 \text{Tr}P_S \\ &= \frac{M(1+\varepsilon^2) + 2\varepsilon}{M(M^2-1)} \end{aligned} \quad (7.30)$$

Using Eq. (3.11) to translate purity to the radius one finds, after some algebra,

$$r(\rho) = r_0^2 \left(1 + \varepsilon\sqrt{N}\right) \quad (7.31)$$

Since partial transposition is an isometry, ρ^{pt} is also near the Gurvits-Barnum ball. It is an entanglement witness for the Bell state:

$$-\varepsilon = \text{Tr}(\rho S) = \text{Tr}(\rho^{pt} S^{pt}) = M \langle \beta | \rho^{pt} | \beta \rangle \quad (7.32)$$

and we have used Eq. (7.24) in the last step.

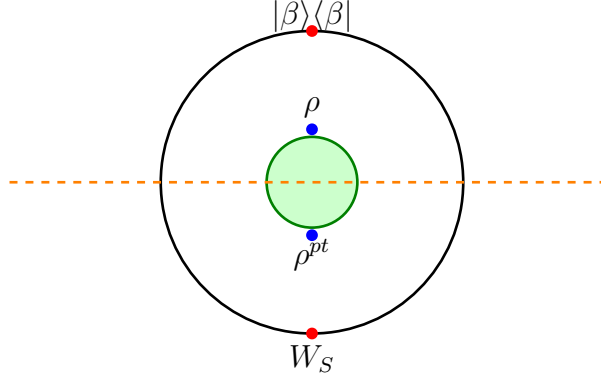


Figure 16: The figure shows the maximally entangled state $|\beta\rangle\langle\beta|$ on the unit circle, its witness ρ^{pt} , the entangled state ρ and the normalized swap witness, W_S . ρ and ρ^{pt} lie close to the boundary of the Gurvits-Barnum ball of separable states. The dashed line represent the reflection plane associated with partial transposition.

7.8 A Clifford ball of separable states

Here we construct a $2\ell - 1$ Clifford ball with radius r_0 , of separable quantum states, in the Hilbert space $\mathbb{C}^N = \mathbb{C}^M \otimes \mathbb{C}^M$. ℓ is the (maximal) number of anti-commuting (generalized) Pauli matrices σ_μ , acting on \mathbb{C}^M . We call this ball the Clifford ball. Its radius is larger than the radius r_0^2 of the Gurvits-Barnum ball, but it lives in a lower dimension.

A standard construction of $2\ell - 1$ anti-commuting Pauli matrices, acting on \mathbb{C}^N , $N = M^2$, from ℓ anti-commuting matrices acting on \mathbb{C}^M is

$$\sigma_\mu \otimes \sigma_\ell, \quad \mathbb{1} \otimes \sigma_\nu, \quad \mu = 1 \dots \ell, \quad \nu = 1 \dots \ell - 1 \quad (7.33)$$

Consider the $2\ell - 1$ dimensional family of quantum states in \mathbb{C}^N , parametrized by \mathbf{a}, \mathbf{b} ¹⁶

$$\rho = \frac{\mathbb{1}_M \otimes \mathbb{1}_M + \mathbf{a} \cdot \boldsymbol{\sigma} \otimes \sigma_\ell + \mathbb{1} \otimes \mathbf{b} \cdot \boldsymbol{\sigma}}{M^2} \geq 0, \quad \mathbf{a}, \mathbf{b} \in \mathbb{R}^\ell, \quad b_\ell = 0 \quad (7.34)$$

where $\boldsymbol{\sigma} = (\sigma_1, \dots, \sigma_\ell)$ is a vector of $M \times M$ (generalized, anti-commuting) Pauli matrices. We shall show that for $\mathbf{a}^2 + \mathbf{b}^2 \leq 1$, ρ is essentially equivalent to a family of 2-qubit states, which are manifestly separable. Re-scaling the \mathbf{a}, \mathbf{b} coordinates to fit with the convention in Eq.(3.1) gives the radius r_0 .

Note first that since

$$(\mathbf{a} \cdot \boldsymbol{\sigma})^2 = a^2 \mathbb{1}_M, \quad \sigma_\ell^2 = \mathbb{1}_M, \quad (\mathbf{b} \cdot \boldsymbol{\sigma})^2 = b^2 \mathbb{1}_M, \quad \{\sigma_\ell, \mathbf{b} \cdot \boldsymbol{\sigma}\} = 0 \quad (7.35)$$

¹⁶Note the change of normalization relative to Eq. (3.1).

we may write

$$\mathbf{a} \cdot \boldsymbol{\sigma} = \mathbb{1}_{M/2} \otimes aZ \quad \sigma_\ell = Z \otimes \mathbb{1}_{M/2}, \quad \mathbf{b} \cdot \boldsymbol{\sigma} = bX \otimes \mathbb{1}_{M/2} \quad (7.36)$$

where Z, X are the standard 2×2 Pauli matrices. The numerator in Eq. (7.34) takes the form

$$\mathbb{1}_{M/2} \otimes \left(\mathbb{1}_2 \otimes \mathbb{1}_2 + aZ \otimes Z + \mathbb{1}_2 \otimes bX \right) \otimes \mathbb{1}_{M/2} \quad (7.37)$$

The brackets can be written as:

$$|0\rangle \langle 0| \otimes (\mathbb{1} + aZ + bX) + |1\rangle \langle 1| \otimes (\mathbb{1} - aZ + bX) \quad (7.38)$$

$(\mathbb{1} \pm aZ + bX) \geq 0$ when $a^2 + b^2 \leq 1$, and the resulting expression for ρ is manifestly separable. Rescaling the coordinates gives the radius r_0 for the Clifford ball of separable state.

Acknowledgement

The research has been supported by ISF. We thank Yuval Lemberg for help in the initial stages of this work and Andrzej Kossakowski for his encouragement.

A The average purity of quantum states

In section 6.2 we quoted a result of [24], Eq. (6.8), which allows to explicitly compute the radius of inertia r_e of D_N as a rational function of N . The aim of this appendix is to give an elementary derivation of this formula.

The measure $d\mu$ on the space of density matrices in section 6.2 is a special case of a more general measures $d\mu_{N,K}$ when $N = K$. The measures $d\mu_{N,K}$ are the induced measure on density matrices acting on \mathbb{C}^N , obtained from the uniform measure on pure states on $\mathbb{C}^N \otimes \mathbb{C}^K$ with $K \geq N$, by partial tracing over the second factor¹⁷. They are all simply related [24]

$$d\mu_{N,K} = \frac{1}{Z_{N,K}} (\det(\rho))^{K-N} dx_1 \dots dx_{N^2-1}, \quad K \geq N \quad (\text{A.1})$$

$Z_{N,K}$ is a normalization factor. The Euclidean measure $d\mu$ corresponds to the case $N = K$.

The derivation given below of Eq. (6.8) is simpler than the original derivation in [24] in that it avoids the constraint associated with the normalization of the wave functions. Using this observation, computing the second moment of \mathbf{x}^2 with respect to the measure $d\mu_{N,K}$ reduces to an exercise in Gaussian integration.

Let $\langle \alpha j | \psi \rangle = \xi_{\alpha j}$ be the amplitudes of the pure state $|\psi\rangle$ in $\mathbb{C}^N \otimes \mathbb{C}^K$. The first factor is the system and the second is the ancilla. The density matrix ρ is obtained by partial tracing the ancilla.

$$\langle \alpha | \rho | \beta \rangle = \langle \alpha | (Tr_K |\psi\rangle \langle \psi|) | \beta \rangle = \sum_j \xi_{\alpha j} \bar{\xi}_{\beta j} = (\xi \xi^*)_{\alpha\beta} \quad (\text{A.2})$$

where ξ is an $N \times K$ matrix. The requirement $K \geq N$ guarantees that (generically) ρ is full rank.

Choosing $Re \xi_{\alpha j}$ and $Im \xi_{\alpha j}$ to be normally distributed i.i.d., gives a uniform measure on pure states, $d\mu_\psi$, which is unitary invariant under $U(NK)$. The induced measure on the density matrices $d\mu_{N,K}$

$$d\mu_{NK} = d\rho \int \delta(\rho - Tr_K |\psi\rangle \langle \psi|) d\mu_\psi \quad (\text{A.3})$$

Since the Gaussian measure for ξ allows for states that are not normalized, the measure $d\mu_{N,K}$ allows for any $Tr \rho \geq 0$. This means that to compute the moments of normalized density matrices we need to compute

$$\int d\mu_{N,K} \frac{Tr \rho^2}{(Tr \rho)^2} \quad (\text{A.4})$$

¹⁷In the case $K = N - 1$ the measure is concentrated on the boundary of D_N being proportional to $\delta(\det \rho)$.

The reason one can explicitly compute such integral is that the measure factors

$$d\mu_{N,K} = d\mu_{|\rho|} \otimes d\mu_{\Omega} \quad (\text{A.5})$$

$Tr\rho = \|\psi\|^2$ depends only on the first, radial, coordinate while $\frac{Tr\rho^2}{(Tr\rho)^2}$ depends only on the second, angular, part

$$\begin{aligned} \int d\mu_{N,K} Tr(\rho^2) &= \int d\mu_{\Omega} \frac{Tr\rho^2}{(Tr\rho)^2} \int d\mu_{|\rho|} (Tr\rho)^2 \\ &= \int d\mu_{N,K} \frac{Tr\rho^2}{(Tr\rho)^2} \int d\mu_{N,K} (Tr\rho)^2 \end{aligned} \quad (\text{A.6})$$

(Assuming $d\mu_{NK}$ normalized.) The integral in Eq. (A.4) is reduced to (ratio of) two Gaussian integrals. Wick theorem (for the standard normal distribution) gives

$$\begin{aligned} \int d\mu_{N,K} Tr(\rho^2) &= \sum_{jk\alpha\beta} \int d\mu_{\psi} \xi_{\alpha j} \bar{\xi}_{\beta j} \bar{\xi}_{\beta k} \xi_{\alpha k} \\ &= \sum_{jk\alpha\beta} (\delta_{\alpha\beta} + \delta_{jk}) \\ &= NK(K+N) \end{aligned} \quad (\text{A.7})$$

Similarly

$$\begin{aligned} \int d\mu_{N,K} (Tr\rho)^2 &= \sum_{jk\alpha\beta} \int d\mu_G \xi_{\alpha j} \bar{\xi}_{\alpha j} \bar{\xi}_{\beta k} \xi_{\beta k} \\ &= \sum_{jk\alpha\beta} (1 + \delta_{jk} \delta_{\alpha\beta}) \\ &= NK(NK+1) \end{aligned} \quad (\text{A.8})$$

So finally,

$$\int d\mu_{N,K} \frac{Tr\rho^2}{(Tr\rho)^2} = \frac{N+K}{KN+1} \quad (\text{A.9})$$

This reduces to Eq. (6.9) when $N=K$.

The computation of higher moments can be similarly reduced to a (tedious) combinatoric problem.

B The N dimensional unit cube is almost a ball

The fact that D_N looks like a ball in most directions is a general fact about convex bodies in high dimensions. It is instructive to see this happening for the unit cube

in N dimensions

$$C = \left\{ \mathbf{x} \mid \mathbf{x} = (x_1, \dots, x_N), \quad |x_j| \leq \frac{1}{2}, \quad j = 1, \dots, N \right\} \quad (\text{B.1})$$

The radius of inertia of C is

$$r_e^2 = \mathbb{E}(\mathbf{x}^2) = \sum \mathbb{E}(x_j^2) = N \int_{-1/2}^{1/2} x^2 dx = \frac{N}{12} \quad (\text{B.2})$$

Let us now consider $r(\theta)$, defined as the maximal r that is inside the cube for a given direction θ .

Choose a random direction $\boldsymbol{\theta} = (\theta_1, \dots, \theta_N)$ by picking θ_j to be normal iid with

$$\theta_j \sim \mathcal{N}\left[0, \frac{1}{N}\right], \quad x_j = r\theta_j \quad (\text{B.3})$$

When N is large there is a “phase transition” in the sense that

$$\text{Prob}(r\boldsymbol{\theta} \in C) \approx \begin{cases} 1 & r < r_C \\ 0 & r > r_C \end{cases}, \quad r_C = \frac{1}{2} \sqrt{\frac{N}{\log N}} \quad (\text{B.4})$$

To see this we first observe that the probability that $x \sim \mathcal{N}(0, \sigma^2)$ takes values outside the interval $[-x_0, x_0]$ is given by the complementary error function

$$\text{Prob}(|x| > x_0) = \sqrt{\frac{2}{\pi}} \int_{x_0/\sigma}^{\infty} e^{-x^2/2} dx = \text{erfc}(x_0/\sigma)$$

Anticipating the result, Eq. (B.4), let us replace r by its re-scaled version k :

$$r = kr_C \quad (\text{B.5})$$

For the case at hand

$$\sigma^2 = 1/N, \quad x_0 = \frac{1}{2r} = \frac{1}{2kr_C}$$

The probability for $r|\theta_j| = |x_j| \leq 1/2$ happening for all coordinates simultaneously is

$$\text{Prob}(r\boldsymbol{\theta} \in C) = \left(1 - \text{erfc}\left(\frac{\sqrt{\log N}}{k}\right)\right)^N$$

Since $\text{erfc}(x) \in [0, 1]$ for $x \in [0, \infty)$, the limit $N \rightarrow \infty$ tends to

$$\text{Prob}(r\boldsymbol{\theta} \in C) \rightarrow \begin{cases} 0 & \text{if } N\text{erfc}\left(\frac{\sqrt{\log N}}{k}\right) \rightarrow \infty \\ 1 & \text{if } N\text{erfc}\left(\frac{\sqrt{\log N}}{k}\right) \rightarrow 0 \end{cases} \quad (\text{B.6})$$

Since

$$N\text{erfc}\left(\frac{\sqrt{\log N}}{k}\right) \rightarrow \begin{cases} \infty & \text{for } k > 1 \\ 0 & \text{for } k \leq 1 \end{cases} \quad (\text{B.7})$$

Eq. (B.4) follows.

References

- [1] Michael A Nielsen and Isaac Chuang. *Quantum computation and quantum information*. AAPT, 2002.
- [2] Ingemar Bengtsson and Karol Życzkowski. *Geometry of quantum states: an introduction to quantum entanglement*. Cambridge university press, 2017.
- [3] Jon Magne Leinaas, Jan Myrheim, and Eirik Ovrum. Geometrical aspects of entanglement. *Phys. Rev. A*, 74:012313, Jul 2006.
- [4] JE Avron and O Kenneth. Entanglement and the geometry of two qubits. *Annals of Physics*, 324(2):470–496, 2009.
- [5] Guillaume Aubrun and Stanisław J Szarek. Alice and bob meet banach. *Mathematical Surveys and Monographs*, 223, 2017.
- [6] Leonid Gurvits and Howard Barnum. Largest separable balls around the maximally mixed bipartite quantum state. *Physical Review A*, 66(6):062311, 2002.
- [7] Madan Lal Mehta. *Random matrices*, volume 142. Elsevier, 2004.
- [8] Noga Alon and Joel Spencer. *The Probabilistic Method*. John Wiley, 1992.
- [9] Stanisław J Szarek. Volume of separable states is super-doubly-exponentially small in the number of qubits. *Physical Review A*, 72(3):032304, 2005.
- [10] G. Milman, V. D. Schechtman. *Asymptotic Theory of Finite-Dimensional Normed Spaces*. Lecture Notes in Mathematics, Vol. 1,200. Springer, 1986.
- [11] Patrick Hayden, Debbie W Leung, and Andreas Winter. Aspects of generic entanglement. *Communications in Mathematical Physics*, 265(1):95–117, 2006.
- [12] A Peres. *Quantum mechanics: concepts and methods*. Kluwer, Dordrecht, 1993.
- [13] Karol Życzkowski, Paweł Horodecki, Anna Sanpera, and Maciej Lewenstein. Volume of the set of separable states. *Phys. Rev. A*, 58:883–892, Aug 1998.
- [14] F Hulpke and D Bru. A two-way algorithm for the entanglement problem. *Journal of Physics A: Mathematical and General*, 38(24):5573, 2005.
- [15] Andrew C. Doherty, Pablo A. Parrilo, and Federico M. Spedalieri. Complete family of separability criteria. *Phys. Rev. A*, 69:022308, Feb 2004.

- [16] Ryszard Horodecki, Paweł Horodecki, Michał Horodecki, and Karol Horodecki. Quantum entanglement. *Reviews of modern physics*, 81(2):865, 2009.
- [17] Erling Størmer. *Positive linear maps of operator algebras*. Springer Science & Business Media, 2012.
- [18] William K. Wootters. Entanglement of formation of an arbitrary state of two qubits. *Phys. Rev. Lett.*, 80:2245–2248, Mar 1998.
- [19] Ryszard Horodecki and Michał Horodecki. Information-theoretic aspects of inseparability of mixed states. *Phys. Rev. A*, 54:1838–1843, Sep 1996.
- [20] Mary Beth Ruskai. Qubit entanglement breaking channels. *Reviews in Mathematical Physics*, 15(06):643–662, 2003.
- [21] Keith Ball et al. An elementary introduction to modern convex geometry. *Flavors of geometry*, 31:1–58, 1997.
- [22] Percy Deift. Universality for mathematical and physical systems. Proceedings of the International Congress of Mathematics, Madrid, Spain *arXiv preprint math-ph/0603038*, 2006.
- [23] Craig A Tracy and Harold Widom. Level-spacing distributions and the airy kernel. *Communications in Mathematical Physics*, 159(1):151–174, 1994.
- [24] Karol Życzkowski and Hans-Jürgen Sommers. Induced measures in the space of mixed quantum states. *Journal of Physics A: Mathematical and General*, 34(35):7111, 2001.
- [25] Lawrence M Ioannou. Computational complexity of the quantum separability problem. *Quantum Information & Computation*, 7(4):335–370, 2007.
- [26] N. Shalev, O. Messer, J. Avron, and O. Kenneth. State separator v2. <http://physics.technion.ac.il/stateseparator/index.html/>.
- [27] Asher Peres. Separability criterion for density matrices. *Phys. Rev. Lett.*, 77:1413–1415, Aug 1996.
- [28] C. H. Bennett, H. J. Bernstein, S. Popescu, and B. Schumacher. Concentrating partial entanglement by local operations. *Phys. Rev. A*, 53:2046–2052, April 1996.
- [29] Charles H Bennett, David P DiVincenzo, Tal Mor, Peter W Shor, John A Smolin, and Barbara M Terhal. Unextendible product bases and bound entanglement. *Physical Review Letters*, 82(26):5385, 1999.